

Slow Wave Phenomena in Photonic Crystals

Alex Figotin and Ilya Vitebskiy

Abstract. The problem of slowing down light by orders of magnitude has been extensively discussed in the literature. Such a possibility can be useful in a variety of optical applications. Many qualitatively different approaches have been explored. Here we discuss how this goal can be achieved in linear dispersive media, such as photonic crystals. The existence of slowly propagating light in photonic crystals is quite obvious and well known. The main problem, though, has been how to effectively convert the input radiation into the slow mode without losing a significant portion of the incident light energy to absorption, reflection, etc. We show that the so-called frozen mode regime offers a unique solution to the above problem. Under the frozen mode regime, the incident light can be completely converted into the frozen mode with huge amplitude and almost zero group velocity. The frozen mode regime is a fundamentally new wave phenomenon – it does not reduce to any known electromagnetic resonance. Formally, the frozen mode regime is not a resonance, in a sense that it is not particularly sensitive to the size and shape of the photonic crystal. The frozen mode regime is much more robust and powerful, compared to any known slow-wave resonance. It has much higher tolerance to absorption and structural imperfections than common Fabry-Perot or transmission band edge resonances, where the entire photonic crystal works as a resonator.

1. Introduction

1.1. What is slow light?

The velocity of light in transparent dispersive media is characterized by two different physical quantities – the phase velocity and the group velocity. The phase velocity of a travelling wave is defined as

$$v_{ph} = \omega/k, \quad (1)$$

where ω is the angular frequency and k is the wave number (the propagation vector). The group velocity of a travelling wave is defined as

$$v_g = \partial\omega/\partial k. \quad (2)$$

The group velocity of light is one of the most important electromagnetic characteristics of transparent medium. It determines the speed of pulse propagation and is usually referred to simply as the speed of light propagation. With certain reservations, the group velocity also coincides with electromagnetic energy velocity in a wave packet [1, 2]. The definitions (1) and (2) apply not only to uniform transparent media and waveguides, but also to nonuniform spatially periodic structures, such as photonic crystals, arrays of coupled optical resonators, etc. In the case of a periodic structure, k is the Bloch wave number defined in the first Brillouin zone [1]. By definition, in a slow light case, the electromagnetic pulse propagates through the dispersive medium with the speed $v_g \ll c$, while the respective value of phase velocity (1) is irrelevant.

The term "slow light" has been widely used to describe a broad range of qualitatively different physical phenomena. There have been hundreds of publications in which the above term appears as a key word, while in many cases, the physical phenomena in question have little in common. Below, we briefly outline the most important situations in which the concept of slow light can be invoked. Most of such cases can be grouped into two major categories:

- those where the low group velocity of light results from strong temporal (frequency) dispersion of the transparent medium;
- those where the low speed of pulse propagation is a result of coherent interference in spatially periodic structures.

1.2. Slow light in media with strong temporal dispersion

In a uniform medium, both the phase and the group velocities of light can be expressed in terms of the refractive index n

$$v_f = c/n, \quad (3)$$

$$v_g = c \left(n + \omega \frac{dn}{d\omega} \right)^{-1}. \quad (4)$$

The derivative $dn/d\omega$ in (4) characterizes the temporal dispersion of the medium. At optical frequencies, the refractive index n of common transparent substances does not exceed several units, and the speed of light propagation is of the same order of magnitude as in vacuum. The situation can change dramatically in a strongly dispersive medium where the term $\omega dn/d\omega$ in (4) becomes dominant

$$\text{if } \omega \frac{dn}{d\omega} \gg n, \quad v_g \approx c \left(\omega \frac{dn}{d\omega} \right)^{-1} \ll c. \quad (5)$$

Strong frequency dependence of the refractive index n implies that the light group velocity can be substantially different from c . The relation (5) yields the following limitation on the slow pulse bandwidth

$$\frac{\Delta\omega}{\omega} < \frac{v_g}{c}, \quad (6)$$

where the assumption is made that the refractive index n within the transparency window is of the order of unity. The condition (6) can also be viewed as a constraint on the minimal propagation speed of a pulse with a given bandwidth $\Delta\omega$.

Usually, the large temporal dispersion (5) is a result of excitation of electronic or some other intrinsic resonances of the medium. This always involves some kind of a delicate resonant light-matter interaction with extremely small bandwidth. For instance, in the well known case of electromagnetically induced transparency [3, 4, 5, 6, 7, 8, 9], the incident light interacts with atomic spin excitations forming the so-called dark-state polaritons. These polaritons propagate slowly through the medium in the form of a sharply compressed pulse, the energy of which is much smaller than that of the incident light pulse. In another example, the slow wave is associated with plasmons, which are electron density waves in gas of mobile electrons of the metal. Plasmons also interact with light forming polaritons. There are many more examples of condensed matter excitations, strongly interacting with light and having low group velocity and relatively low relaxation rate. In most of such cases, the slow pulse propagating through the dispersive medium can be seen as an intrinsic coherent excitation (a polariton) triggered by the input light, rather than a light pulse per se. The group velocity of such an excitation may have little to do with the speed of light c .

In the rest of the paper we focus exclusively on the cases not involving any intrinsic excitations of the medium and, therefore, not related to temporal dispersion. Instead, we will focus on spatially periodic structures, in which low speed of electromagnetic pulse propagation results solely from spatial inhomogeneity.

1.3. Slow light in spatially periodic structures

Well-known examples of periodic dielectric structures include photonic crystals [10], periodic arrays of coupled optical resonators [11, 12, 13, 14, 15, 16, 17], and line-defect waveguides [25]. Low speed of pulse propagation in all these cases is the result of coherent interference of light scattered at the interfaces between adjacent structural components. The effects of spatial dispersion associated with structural periodicity are particularly strong when the structural period L and the light wavelength λ are comparable in value

$$L \sim \lambda. \quad (7)$$

Strong spatial dispersion can result in low or even zero group velocity of the respective Bloch wave. In practice, at optical frequencies, the speed of pulse propagation in periodic dielectric arrays can be reduced by not more than three orders of magnitude. This is not a fundamental restriction, but rather a technological limitation related to the difficulty of building flawless periodic arrays at nanoscales. On the positive side, the dielectric components of the periodic array are not required to display strong temporal dispersion. As a consequence, the absorption of light is not an inherent problem in this case.

There is a natural bandwidth limitation on the slowed pulse in periodic dielectric arrays, which is similar to the case of slow light in time-dispersive media. Let $\Delta\omega$ be the frequency bandwidth of a pulse and Δk – the respective range of the Bloch wave number. The average group velocity $\langle v_g \rangle$ of the pulse can be defined as

$$\langle v_g \rangle \approx \frac{\Delta\omega}{\Delta k}. \quad (8)$$

Let us assume that the pulse propagating in the periodic medium is composed of the Bloch eigenmodes belonging to the same spectral branch of the dispersion relation $\omega(k)$. This assumption implies that Δk cannot exceed the size $2\pi/L$ of the Brillouin zone

$$\Delta k < 2\pi/L,$$

where L is the unit cell length of the periodic array. In addition, we assume that the refractive index of the constitutive components of the periodic array is of the order of unity and, therefore,

$$L \sim \lambda_0 = 2\pi c/\omega, \quad (9)$$

where λ_0 is the light wavelength in vacuum. The relations (8) and (9) yield the following limitation on the minimal propagation speed of a pulse with a given bandwidth $\Delta\omega$

$$\langle v_g \rangle > \frac{L}{2\pi} \Delta\omega \sim c \frac{\Delta\omega}{\omega}. \quad (10)$$

The restriction (10) is similar to that defined by the inequality (6) and related to the case of slow light in a uniform medium with temporal (frequency) dispersion.

1.4. Examples of periodic arrays supporting slow light

1.4.1. Coupled resonator optical waveguide During the last two decades, a tremendous progress has been made in theory and applications of periodic arrays of coupled optical resonators. Generally, if the coupling between adjacent resonators in a periodic array is weak, the group velocity of Bloch excitations propagating through the array is very low in each and every transmission band. This is true regardless of the nature of individual resonators. The above simple and general idea forms the basis for one of the most popular approaches to slowing down the light. One inevitable consequence of the weak coupling between the neighboring resonators is that all the individual transmission bands are very narrow. Another problem is that there can be severe restrictions on transmitted power. An extensive discussion on the subject and numerous examples and references can be found in [11] [11, 12, 13, 14, 15, 16, 17]. A qualitatively similar situation occurs in line-defect waveguides in a photonic crystal slab, where a periodic array of structural defects plays the role of weakly coupled optical resonators [25].

Slow light phenomena in periodic arrays of weakly coupled resonators have been the subject of a great number of recent publications, including some excellent review articles cited above. A common characteristic of all different realizations of this approach is a relatively low density of modes. One consequence of this is a significant nonlinearity. In certain cases, the nonlinearity is so extreme that it occurs even on a single photon level. Strong nonlinearity can be useful in controlling the flow of light. On the other hand, it can severely limit the transmission capabilities of the optical waveguide. In this respect, photonic crystals are of great advantage.

1.4.2. Photonic crystals. Photonic crystals are spatially periodic structures composed of two or more different transparent dielectric materials [10]. Strong spatial dispersion of a typical photonic crystal is reflected in a complicated $k - \omega$ diagram featuring transmission bands and gaps. Normally, each spectral branch $\omega(k)$ of the Bloch dispersion relation develops stationary points $\omega_s = \omega(k_s)$ where the group velocity (2) of the corresponding propagating mode vanishes

$$d\omega/dk = 0, \text{ at } \omega = \omega_s = \omega(k_s). \quad (11)$$

Examples of different stationary points are shown in Fig. 1, where each of the frequencies ω_g , ω_0 and ω_d is associated with zero group velocity of the respective traveling wave.

Unlike the case of optical waveguides and linear arrays of coupled resonators, in photonic crystals we have bulk electromagnetic waves capable of propagating in any direction through the periodic heterogeneous structure. This results in much greater density of modes, compared to arrays of weakly coupled resonators.

A major problem with slow light in photonic crystals is the efficiency of conversion of the incident light into the slow mode inside the heterogeneous medium. In most cases, an incident electromagnetic wave with the frequency of one of the slow modes is simply reflected back to space, without creating the slow mode inside the photonic crystal. How to overcome this fundamental problem and, thereby, how to transform a significant fraction of the incident light energy into a slow mode with drastically enhanced amplitude, is the primary subject of this paper.

2. Frozen mode regime in photonic crystals.

The effects of strong spatial dispersion in periodic dielectric structures culminate at stationary points (11) of the Bloch dispersion relation, where the group velocity (2) of a traveling Bloch wave vanishes. One reason for this is that vanishing group velocity always implies a dramatic increase in density of modes at the respective frequency. In addition, vanishing group velocity also implies certain qualitative changes in the eigenmode structure, which can be accompanied by some spectacular effects in electromagnetic wave propagation. A particular example of the kind is the frozen mode regime associated with a dramatic enhancement of the wave transmitted to the periodic medium [39, 29, 30, 31, 35]. There are at least two qualitatively different modifications of the frozen mode regime, each related to a specific singularity of the electromagnetic dispersion relation. Both effects can be explained using the simple example of a plane electromagnetic wave normally incident on a lossless semi-infinite periodic structure.

The frozen mode regime of the first kind is associated with a stationary inflection point (SIP) on the $k - \omega$ diagram shown in Fig. 1(b). In the vicinity of stationary inflection point, the relation between the frequency ω and the Bloch wave number k can be approximated as

$$\omega - \omega_0 \propto (k - k_0)^3. \quad (12)$$

A monochromatic plane wave of frequency close to ω_0 incident on semi-infinite photonic crystal is converted into the frozen mode with infinitesimal group velocity and dramatically enhanced amplitude, as illustrated in Fig. 2. The saturation value of the frozen mode amplitude diverges as the frequency approaches its critical value ω_0 . Remarkably, the photonic crystal reflectivity at $\omega = \omega_0$ can be very low, implying

that the incident radiation is almost totally converted into the frozen mode with zero group velocity, diverging amplitude, and finite energy flux close to that of the incident wave.

A qualitatively different kind of frozen mode regime is expected in the vicinity of a degenerate photonic band edge (DBE) shown in Fig. 1(c). At frequencies just below ω_d , the dispersion relation can be approximated as

$$\omega_d - \omega \propto (k - k_d)^4, \text{ at } \omega \lesssim \omega_d. \quad (13)$$

Contrary to the case of stationary inflection point (12), in the vicinity of a degenerate band edge the photonic crystal becomes totally reflective. But at the same time, the steady-state field inside the periodic medium (at $z > 0$) develops a very large amplitude, diverging as the frequency approaches its critical value ω_d . Such a behavior is illustrated in Fig. 3. The frozen mode profile below and above the degenerate band edge frequency ω_d is different. It has a large saturation value at frequencies located inside the transmission band (at $\omega \leq \omega_d$), as seen in Fig. 3(a) and (b). This saturation value diverges as $\omega \rightarrow \omega_d - 0$. By contrast, at frequencies inside the band gap (at $\omega > \omega_d$), the field amplitude initially increases dramatically with the distance z from the surface, but then vanishes as the distance z further increases, as seen in Fig. 3(d – f).

Hereinafter, the above phenomena will be referred to as the SIP-related frozen mode regime and the DBE-related frozen mode regime, respectively.

Fig. 2 describes the SIP-related frozen mode regime in hypothetical lossless semi-infinite periodic media. In the case of a plane-parallel photonic sample with finite thickness, the frozen mode profile remains unchanged in the leftmost portion of the periodic structure. In the opposite, rightmost part of the photonic crystal, the frozen mode amplitude vanishes, as illustrated in Fig. 4. Additional factors limiting the frozen mode amplitude include structural imperfections of the periodic array, absorption, nonlinearity, deviation of the incident radiation from plane monochromatic wave, etc.

In the case of DBE-related frozen mode regime, the situation is quite different. Specifically, in the case of plane-parallel photonic sample with finite thickness, the DBE-related frozen mode regime becomes overwhelmed with much more powerful, giant slow wave resonance [33, 34].

Not every periodic structure can support the frozen mode regime at normal incidence. Generally, the physical conditions for the frozen mode regime are the same as the conditions for the existence of the respective stationary point (12) or (13) of the dispersion relation. For instance, in the case, of periodic layered structures, a unit cell must contain at least three layers, of which two must display a misaligned in-plane anisotropy [39, 29, 32].

The frozen mode regime is a fundamentally new wave phenomenon – it does not reduce to any known electromagnetic resonance. Formally, the frozen mode regime is not a resonance, in a sense that it is not particularly sensitive to the size and shape of the photonic crystal. Besides, the frequency dependence of the frozen mode amplitude is very different from that of a cavity or a common slow wave resonance. The frozen mode regime is much more robust and powerful, compared to any known slow-wave resonance occurring in periodic and nonperiodic photonic structures. It has much higher tolerance to absorption and structural imperfections than common Fabry-Perot or transmission band edge resonances, where the entire photonic crystal works as a resonator. On the other hand, it is possible to combine the DBE-related frozen mode

regime and a slow wave optical resonance, in which case we have the phenomenon called the giant slow-wave resonance [33, 34]. The quality factor associated with such a resonance can be by two orders of magnitude higher, compared to that of the regular slow-wave resonance in the same or similar periodic structure. More importantly, the frozen mode regime provides the possibility of a dramatic reduction in size – up to an order of magnitude – of some basic photonic devices without compromising on their performance.

3. The physical nature of the frozen mode regime

The essence of the frozen mode regime can be understood from the simple example of a plane monochromatic wave normally incident on a semi-infinite periodic layered structure. An important requirement, though, is that some of the layers display a misaligned in-plane anisotropy [39, 29, 32]. Below we present a comparative analysis of two different kinds of frozen mode regime. Although throughout this section we only consider the case of normal incidence, most of the results and expressions remain virtually unchanged in a more general case of the frozen mode regime at oblique propagation [30, 31, 32]. One difference, though, is that at oblique incidence, the frozen mode regime can occur in much simpler structures. This can have a big practical advantage.

To start with, let us introduce some basic notations and definitions. Let Ψ_I , Ψ_R , and Ψ_T be the incident, reflected and transmitted waves, respectively. Assume for now that all three monochromatic waves propagate along the z axis normal to the surface of semi-infinite periodic structure. Electromagnetic field both inside (at $z > 0$) and outside (at $z < 0$) the photonic structure is independent of the x and y coordinates. The transverse field components can be represented as a column-vector

$$\Psi(z) = \begin{bmatrix} E_x(z) \\ E_y(z) \\ H_x(z) \\ H_y(z) \end{bmatrix}, \quad (14)$$

where $\vec{E}(z)$ and $\vec{H}(z)$ are time-harmonic electric and magnetic fields. All four transverse field components in (14) are continuous functions of z , which leads to the following standard boundary condition at $z = 0$

$$\Psi_T(0) = \Psi_I(0) + \Psi_R(0). \quad (15)$$

Assume also that anisotropic layers of the periodic array have an in-plane anisotropy, in which case the fields $\vec{E}(z)$ and $\vec{H}(z)$ are normal to the direction of propagation

$$\vec{E}(z) \perp z, \vec{H}(z) \perp z, \quad (16)$$

and the column vector (14) includes all nonzero field components. Note that the polarizations of the incident, reflected and transmitted waves can be different, because some of the layers of the periodic array display an in-plane anisotropy. The presence of anisotropic layers is essential for the possibility of frozen mode regime.

In periodic layered media, the electromagnetic eigenmodes $\Psi_k(z)$ are usually chosen in the Bloch form

$$\Psi_k(z + L) = e^{ikL} \Psi_k(z), \quad (17)$$

where the Bloch wave number k is defined up to a multiple of $2\pi/L$. The correspondence between ω and k is referred to as the Bloch dispersion relation. Real k correspond to propagating (traveling) Bloch modes. Propagating modes belong to different spectral branches $\omega(k)$ separated by frequency gaps. The speed of a traveling wave in a periodic medium is determined by the group velocity (2).

By contrast, evanescent Bloch modes are characterized by complex wave numbers $k = k' + ik''$. Evanescent modes decay exponentially with the distance z from the boundary of semi-infinite periodic structure. Therefore, under normal circumstances, evanescent contribution to the transmitted wave $\Psi_T(z)$ can be significant only in close proximity of the surface. The situation can change dramatically when the frequency ω approaches one of the stationary point values ω_s . At first sight, stationary points (11) relate only to propagating Bloch modes. But in fact, in the vicinity of every stationary point frequency ω_s , the imaginary part k'' of the Bloch wave number of at least one of the evanescent modes also vanishes. As a consequence, the respective evanescent mode decays very slowly, and its role may extend far beyond the photonic crystal boundary. In addition, in the special cases of interest, the electromagnetic field distribution $\Psi(z)$ in the coexisting evanescent and propagating eigenmodes becomes very similar, as ω approaches ω_s . This can result in spectacular resonance effects, such as the frozen mode regime. What exactly happens in the vicinity of a particular stationary point (11) essentially depends on its character and appears to be very different in each of the three cases presented in Fig. 1.

3.1. Bloch composition of frozen mode

In a periodic layered structure, at any given frequency ω , there are four electromagnetic eigenmodes with different polarizations and wave numbers. But in the setting where the semi-infinite periodic array occupies the half-space $z \geq 0$, the transmitted wave is a superposition of only two of the four Bloch eigenmodes. Indeed, neither the propagating modes with negative group velocity, nor evanescent modes exponentially growing with the distance z from the surface, contribute to $\Psi_T(z)$ in this case. Generally, one can distinguish three different possibilities.

- (i) Both Bloch components of the transmitted wave Ψ_T are propagating modes

$$\Psi_T(z) = \Psi_{pr1}(z) + \Psi_{pr2}(z), \quad z \geq 0. \quad (18)$$

$\Psi_{pr1}(z)$ and $\Psi_{pr2}(z)$ are two propagating Bloch modes with different real wave numbers k_1 and k_2 and different group velocities $u_1 > 0$ and $u_2 > 0$. This constitutes the phenomenon of double refraction, provided that u_1 and u_2 are different. The other two Bloch components of the same frequency have negative group velocities and cannot contribute to the transmitted wave Ψ_T .

- (ii) Both Bloch components of Ψ_T are evanescent

$$\Psi_T(z) = \Psi_{ev1}(z) + \Psi_{ev2}(z), \quad z \geq 0. \quad (19)$$

The respective two values of k are complex with positive imaginary parts $k'' > 0$. This is the case when the frequency ω falls into photonic band gap at $\omega > \omega_g$ in Fig. 1(a) or at $\omega > \omega_d$ in Fig. 1(c). The fact that $k'' > 0$ implies that the wave amplitude decays with the distance z from the surface. In the case (19), the incident wave is totally reflected back to space by the semi-infinite periodic structure.

- (iii) One of the Bloch components of the transmitted wave Ψ_T is a propagating mode with $u > 0$, while the other is an evanescent mode with $k'' > 0$

$$\Psi_T(z) = \Psi_{pr}(z) + \Psi_{ev}(z), \quad z \geq 0. \quad (20)$$

For example, this is the case at $\omega \sim \omega_0$ in Fig. 1(b), as well as at $\omega < \omega_g$ in Fig. 1(a) and at $\omega < \omega_d$ in Fig. 1(c). As the distance z from the surface increases, the evanescent contribution Ψ_{ev} in (20) decays as $\exp(-zk'')$, and the resulting transmitted wave $\Psi_T(z)$ turns into a single propagating Bloch mode Ψ_{pr} .

Propagating modes with $v_g > 0$ and evanescent modes with $k'' > 0$ are referred to as *forward* waves. Only forward modes contribute to the transmitted wave $\Psi_T(z)$ in the case of a periodic semi-infinite stack. The propagating modes with $v_g < 0$ and evanescent modes with $k'' < 0$ are referred to as *backward* waves. The backward waves never contribute to the transmitted wave Ψ_T inside the periodic semi-infinite stack. This statement is based on the following two assumptions:

- The transmitted wave Ψ_T and the reflected wave Ψ_R are originated from the plane wave Ψ_I incident on the semi-infinite photonic slab from the left.
- The periodic structure occupies the entire half-space and is perfectly periodic at $z > 0$.

If either of the above conditions is violated, the electromagnetic field inside the periodic stack can be a superposition of four Bloch eigenmodes with either sign of the group velocity u of propagating contributions, or either sign of k'' of evanescent contributions. This would be the case if the periodic had some kind of structural defects or a finite thickness. At the end of this section we briefly discuss how it would affect the frozen mode regime.

Note also that the assumption that the transmitted wave $\Psi_T(z)$ is a superposition of propagating and/or evanescent Bloch eigenmodes may not apply if the frequency ω exactly coincides with one of the stationary point frequencies (11). For example, at frequency ω_0 of stationary inflection point (12), there are no evanescent solutions to the Maxwell equations, and the transmitted wave $\Psi_T(z)$ is a (non-Bloch) Floquet eigenmode linearly growing with z [29, 30]. Similar situation occurs at frequency ω_d of degenerate band edge (13). The term "non-Bloch" means that the respective field distribution does not comply with the relation (17). At the same time, at any general frequency, including the vicinity of any stationary point (11), the transmitted wave $\Psi_T(z)$ is a superposition of two Bloch eigenmodes, each of which is either propagating, or evanescent.

In all three cases (18 – 20), the contribution of a particular Bloch eigenmode to the transmitted wave Ψ_T depends on the polarization Ψ_I of the incident wave. One can always choose some special incident wave polarization, such that only one of the two forward Bloch modes is excited and the transmitted wave Ψ_T is a single Bloch eigenmode. In the next subsection we will see that there is no frozen mode regime in the case of a single mode excitation. This fact relates to the very nature of the frozen mode regime.

Knowing the Bloch composition of the transmitted wave we can give a semi-qualitative description of what happens when the frequency ω of the incident wave approaches one of the stationary points (11) in Fig. 1.

3.1.1. Regular photonic band edge We start with the simplest case of a regular photonic band edge. There are two different possibilities in this case, but none of them is associated with the frozen mode regime. The first one relates to the trivial case where none of the layers of the periodic structure displays an in-plane anisotropy or gyrotropy. As the result, all eigenmodes are doubly degenerate with respect to polarization. A detailed description of this case can be found in the extensive literature on optics of stratified media [36, 37]. Slightly different scenario occurs if some of the layers are anisotropic or gyrotropic and, as a result, the polarization degeneracy is lifted. Just below the band edge frequency ω_g in Fig. 1(a), the transmitted field $\Psi_T(z)$ is a superposition (20) of one propagating and one evanescent Bloch modes. Due to the boundary condition (15), the amplitude of the transmitted wave at $z = 0$ is comparable to that of the incident wave. In the case of a generic polarization of the incident light, the amplitudes of the propagating and evanescent Bloch components at $z = 0$ are also comparable to each other and to the amplitude of the incident light

$$|\Psi_{pr}(0)| \sim |\Psi_{ev}(0)| \sim |\Psi_I|, \text{ at } \omega \leq \omega_g. \quad (21)$$

As the distance z from the surface increases, the evanescent component $\Psi_{ev}(z)$ decays rapidly, while the amplitude of the propagating component remains constant. Eventually, at a certain distance from the slab surface, the transmitted wave $\Psi_T(z)$ becomes very close to the propagating mode

$$\Psi_T(z) \approx \Psi_{pr}(z), \text{ at } z \gg L, \omega \leq \omega_g. \quad (22)$$

The evanescent component Ψ_{ev} of the transmitted wave does not display any singularity at the band edge frequency ω_g . The propagating mode Ψ_{pr} does develop a singularity associated with vanishing group velocity at $\omega \rightarrow \omega_g - 0$, but its amplitude remains finite and comparable to that of the incident wave. At $\omega > \omega_g$, this propagating mode turns into another evanescent mode in (19). The bottom line is that none of the Bloch components of the transmitted wave develops a large amplitude in the vicinity of a regular photonic band edge. There is no frozen mode regime in this trivial case.

3.1.2. Stationary inflection point A completely different situation develops in the vicinity of a stationary inflection point (12) of the dispersion relation. At $\omega \approx \omega_0$, the transmitted wave Ψ_T is a superposition (20) of one propagating and one evanescent Bloch component. In contrast to the case of a regular photonic band edge, in the vicinity of ω_0 both Bloch contributions to Ψ_T develop strong singularity. Specifically, as the frequency ω approaches ω_0 , both contributions grow dramatically, while remaining nearly equal and opposite in sign at the slab boundary [29]

$$\Psi_{pr}(0) \approx -\Psi_{ev}(0) \propto |\omega - \omega_0|^{-1/3}, \text{ as } \omega \rightarrow \omega_0. \quad (23)$$

Due to the destructive interference (23), the resulting field

$$\Psi_T(0) = \Psi_{pr}(0) + \Psi_{ev}(0)$$

at the surface at $z = 0$ is small enough to satisfy the boundary condition (15). As the distance z from the slab boundary increases, the destructive interference becomes less effective – in part because the evanescent contribution decays exponentially

$$\Psi_{ev}(z) \approx \Psi_{ev}(0) \exp(-zk''), \quad (24)$$

while the amplitude of the propagating contribution remains constant and very large. Eventually, the transmitted wave $\Psi_T(z)$ reaches its large saturation value corresponding to its propagating component Ψ_{pr} , as seen in Fig. 5(a).

Note that the imaginary part k'' of the evanescent mode wave number in (24) also vanishes in the vicinity of stationary inflection point

$$k'' \propto |\omega - \omega_0|^{1/3}, \text{ as } \omega \rightarrow \omega_0, \quad (25)$$

reducing the rate of decay of the evanescent contribution (24). As a consequence, the resulting amplitude $\Psi_T(z)$ of the transmitted wave reaches its large saturation value Ψ_{pr} in (23) only at a certain distance Z from the surface

$$Z \propto 1/k'' \propto |\omega - \omega_0|^{-1/3}. \quad (26)$$

This characteristic distance diverges as the frequency approaches its critical value ω_0 .

If the frequency of the incident wave is exactly equal to the frozen mode frequency ω_0 , the transmitted wave $\Psi_T(z)$ does not reduce to the sum (20) of propagating and evanescent contributions, because at $\omega = \omega_0$, there is no evanescent solutions to the Maxwell equations. Instead, $\Psi_T(z)$ corresponds to a non-Bloch Floquet eigenmode diverging linearly with z [29].

$$\Psi_T(z) - \Psi_T(0) \propto z\Psi_0, \text{ at } \omega = \omega_0. \quad (27)$$

Such a solution is shown in Fig. 2(c).

3.1.3. Degenerate band edge While the situation with a regular photonic band edge appears trivial, the case of a degenerate band edge (13) proves to be quite different. Just below the degenerate band edge frequency ω_d (inside the transmission band), the transmitted field is a superposition (20) of one propagating and one evanescent components. Above ω_d (inside the band gap), the transmitted wave is a combination (19) of two evanescent components. In this respect, a regular and a degenerate band edges are similar to each other. A crucial difference, though, is that in the vicinity of a degenerate band edge, both Bloch contributions to the transmitted wave diverge as ω approaches ω_d , both above and below the band edge frequency. This constitutes the frozen mode regime.

Let us start with the transmission band. As the frequency ω approaches $\omega_d - 0$, both Bloch contributions in (20) grow sharply, while remaining nearly equal and opposite in sign at the surface

$$\Psi_{pr}(0) \approx -\Psi_{ev}(0) \propto |\omega_d - \omega|^{-1/4}, \text{ as } \omega \rightarrow \omega_d - 0. \quad (28)$$

The destructive interference (28) ensures that the boundary condition (15) can be satisfied, while both Bloch contributions to $\Psi_T(z)$ diverge. As the distance z from the slab boundary increases, the evanescent component $\Psi_{ev}(z)$ dies out

$$\Psi_{ev}(z) \approx \Psi_{ev}(0) \exp(-zk'') \quad (29)$$

while the propagating component $\Psi_{pr}(z)$ remains constant and very large. Eventually, as the distance z further increases, the transmitted wave $\Psi_T(z)$ reaches its large saturation value corresponding to its propagating component $\Psi_{pr}(z)$, as illustrated in

Fig. 6. Note that the imaginary part k'' of the evanescent mode wave number also vanishes in the vicinity of degenerate band edge

$$k'' \propto |\omega - \omega_d|^{1/4}, \text{ as } \omega \rightarrow \omega_d, \quad (30)$$

reducing the rate of decay of the evanescent contribution (29). As a consequence, the resulting amplitude $\Psi_T(z)$ of the transmitted wave reaches its large saturation value Ψ_{pr} only at a certain distance Z from the surface

$$Z \propto 1/k'' \propto |\omega - \omega_d|^{-1/4}. \quad (31)$$

This characteristic distance increases as the frequency approaches its critical value ω_d , as illustrated in Fig. 3(a) and (b).

If the frequency ω of the incident wave is exactly equal to ω_d , the transmitted wave $\Psi_T(z)$ does not reduce to the sum of two Bloch contributions. Instead, it corresponds to a non-Bloch Floquet eigenmode linearly diverging with z

$$\Psi_T(z) - \Psi_T(0) \propto z\Psi_d, \text{ at } \omega = \omega_d. \quad (32)$$

This situation is shown in Fig. 3(c).

The above behavior appears to be very similar to that of the frozen mode regime at a stationary inflection point, shown in Figs. 2 and 5. Yet, there is a crucial difference between the frozen mode regime at a stationary inflection point and at a degenerate band edge. In the immediate proximity of a degenerate band edge, the Pointing vector S_T of the transmitted wave is infinitesimal, in spite of the diverging wave amplitude. In other words, although the energy density $W_T \propto |\Psi_T|^2$ of the frozen mode diverges as $\omega \rightarrow \omega_d - 0$, it does not grow fast enough to offset the vanishing group velocity. As a consequence, the photonic crystal becomes totally reflective at $\omega = \omega_d$. Of course, the total reflectivity persists at $\omega > \omega_d$, where there is no propagating modes at all. By contrast, in the case (27) of a stationary inflection point, the respective Pointing vector S_T is finite and can be even close to that of the incident wave, implying low reflectivity and nearly total conversion of the incident wave energy into the frozen mode.

The character of frozen mode regime is different when we approach the degenerate band edge frequency from the band gap. In such a case, the transmitted field $\Psi_T(z)$ is a superposition (19) of two evanescent components. As the frequency ω approaches ω_d , both evanescent contributions grow sharply, while remaining nearly equal and opposite in sign at the photonic crystal boundary

$$\Psi_{ev1}(0) \approx -\Psi_{ev2}(0) \propto |\omega_d - \omega|^{-1/4}, \text{ as } \omega \rightarrow \omega_d + 0. \quad (33)$$

Again, the destructive interference (33) ensures that the boundary condition (15) is satisfied, while both evanescent contributions to $\Psi_T(z)$ diverge in accordance with (33). As the distance z from the slab boundary increases, the destructive interference of these two evanescent components is lifted and the resulting field amplitude increases sharply, as seen in Fig. 7(a). But eventually, as the distance z further increases, the transmitted wave $\Psi_T(z)$ completely decays, because both Bloch contributions to $\Psi_T(z)$ are evanescent. The latter constitutes the major difference between the frozen mode regime above and below the DBE frequency ω_d . The rate of the amplitude decay, as well as the position of the maximum of the transmitted wave amplitude in Figs. 3(d – f) and 7(a), are characterized by the distance Z in (31).

3.1.4. Physical reason for the growing wave amplitude If the frequency ω is close, but not equal, to that of a stationary point (11) of the dispersion relation, the wave $\Psi_T(z)$ transmitted to the semi-infinite periodic layered medium is a superposition of two forward Bloch modes $\Psi_1(z)$ and $\Psi_2(z)$

$$\Psi_T(z) = \Psi_1(z) + \Psi_2(z). \quad (34)$$

The two Bloch modes in (34) can be a propagating and an evanescent, as in (20), or they can be both evanescent, as in (19). In the vicinity of frozen mode regime, as the frequency approaches its critical value (ω_0 or ω_d), the two Bloch eigenmodes contributing to $\Psi_T(z)$ become nearly indistinguishable from each other

$$\Psi_1(z) \approx \alpha \Psi_2(z), \quad \text{as } \omega \rightarrow \omega_s, \quad (35)$$

where α is a scalar, and ω_s is the frozen mode frequency (ω_0 or ω_d). The asymptotic relation (35) reflects a basic property of the transfer matrix of periodic layered structures at frequency of either a stationary inflection point, or a degenerate band edge (see [30, 31, 32]).

Let us show under what circumstances the property (35) can lead to the frozen mode regime. The sum (34) of two nearly parallel column vectors Ψ_1 and Ψ_2 must match the boundary conditions (15) with the incident and reflected waves. If the incident wave polarization is general, then the nearly parallel Bloch components Ψ_1 and Ψ_2 must be very large and nearly equal and opposite

$$\Psi_1(0) \approx -\Psi_2(0), \quad |\Psi_1(0)| \approx |\Psi_2(0)| \gg |\Psi_I|, \quad (36)$$

in order to satisfy the boundary conditions (15). Indeed, since the incident field polarization is general, we have no reason to expect that the column vector $\Psi(0)$ at the surface is nearly parallel to $\Psi_1(0)$ and $\Psi_2(0)$. But on the other hand, the boundary conditions say that

$$\Psi(0) = \Psi_1(0) + \Psi_2(0) \quad (37)$$

Obviously, the only situation where the sum (37) of two nearly parallel vectors can be not nearly parallel to either of them is the one described in (36).

There is one exception, though. As we already stated in (35), in the vicinity of the frozen mode frequency, the two Bloch components Ψ_1 and Ψ_2 of the transmitted wave are nearly parallel to each other. For this reason, if the polarization of the incident wave Ψ_I is such that $\Psi(0)$ in (37) is nearly parallel to one of the Bloch eigenmodes $\Psi_1(0)$ or $\Psi_2(0)$, it is also nearly parallel to the other one. So, all three column vectors $\Psi_1(0)$, $\Psi_2(0)$, and $\Psi(0)$ are now parallel to each other. In this, and only this case, the amplitude of the transmitted wave $\Psi_T(z)$ will be comparable to that of the incident wave. There is no frozen mode regime for the respective vanishingly small range of the incident wave polarization. A particular case of the above situation is a regime of a single mode excitation, where only one of the two Bloch components Ψ_1 or Ψ_2 in (34) contributes to the transmitted wave.

Finally, let us reiterate that in the limiting cases of $\omega = \omega_0$ or $\omega = \omega_d$, the transmitted wave $\Psi_T(z)$ corresponds to the non-Bloch Floquet eigenmode (27) or (32), respectively. Either of them linearly diverges with z . Again, the only exception is when the incident wave has the unique polarization, at which the transmitted wave $\Psi_T(z)$ is a propagating Bloch eigenmode with zero group velocity and a limited amplitude, comparable to that of the incident wave. Incident wave with any other polarization will generate the frozen mode inside the periodic medium.

4. Summary

Although the existence of slow electromagnetic modes in photonic crystals is quite obvious, the next question is whether and how such modes can be excited by incident light. We have shown that two different modifications of the so-called frozen mode regime provides unique advantages in this respect. Generally, the possibility of the frozen mode regime is determined by the character of the Bloch dispersion relation of the periodic structure.

Acknowledgment and Disclaimer: Effort of A. Figotin and I. Vitebskiy is sponsored by the Air Force Office of Scientific Research, Air Force Materials Command, USAF, under grant number FA9550-04-1-0359.

- [1] L. Brillouin. *Wave Propagation and Group Velocity*. (Academic, New York, 1960).
- [2] L. D. Landau, E. M. Lifshitz, L. P. Pitaevskii. *Electrodynamics of continuous media*. (Pergamon, N.Y. 1984).
- [3] S. E. Harris. *Electromagnetically induced transparency*. *Physics Today* **50**, # 7, 36 (1997).
- [4] L. Hau, S. Harris, Z. Dutton, C. Behroozi. *Light speed reduction to 17 metres per second in an ultracold atomic gas*. *Nature*, **397**, 594 – 598, (1999).
- [5] M. Kash, V. Sautenkov, Al. Zibrov, L. Hollberg, G. Welch, M. Lukin, Yu. Rostovtsev, E. Fry, and M. Scully. *Ultraslow Group Velocity and Enhanced Nonlinear Optical Effects in a Coherently Driven Hot Atomic Gas*. *Phys. Rev. Lett.* **82**, #26, 5229 – 5232 (1999)
- [6] D. Budker, D. F. Kimball, S. M. Rochester, and V. V. Yashchuk. *Nonlinear Magneto-optics and Reduced Group Velocity of Light in Atomic Vapor with Slow Ground State Relaxation*. *Phys. Rev. Lett.* **83**, # 9, 1767 (1999).
- [7] M. Lukin and A. Imamoglu. *Controlling photons using electromagnetically induced transparency*. *Nature*, **413**, 273 – 276, (2001).
- [8] D. F. Phillips, A. Fleischhauer, A. Mair, and R. L. Walsworth, M. D. Lukin. *Storage of Light in Atomic Vapor*. *Phys. Rev. Lett.* **86**, # 5, 783 – 786, (2001).
- [9] A.V. Turukhin, V. S. Sudarshanam, M. S. Shahriar, J. A. Musser, B. S. Ham, and P. R. Hemmer. *Observation of Ultraslow and Stored Light Pulses in a Solid*. *Phys. Rev. Lett.* **88**, # 2, 023602 (2002).
- [10] J. Joannopoulos, R. Meade, and J. Winn. *Photonic Crystals*. (Princeton University Press, 1995).
- [11] J. Heebner and R. Boyd. *Slow and stopped light*. ‘Slow’ and ‘fast’ light in resonator-coupled waveguides. *Journal of modern optics*, **49**, #14/15, 2629 (2002).
- [12] J. Heebner and R. Boyd. *Slow light, induced dispersion, enhanced nonlinearity, and optical solitons in a resonator-array waveguide*. *Phys. Rev. E***65**, 036619 (2002).
- [13] A. Melloni, F. Morichetti, M. Maritelli. *Linear and nonlinear pulse propagation in coupled resonator slow-wave optical structures*. *Optical and Quantum Electronics* **35**, 365 (2003)
- [14] J. Poon, J. Scheuer, Y. Xu, and A. Yariv. *Designing coupled-resonator optical waveguide delay lines*. *J. Opt. Soc. Am. B*, Vol. **21**, No. 9 (2004).
- [15] J. Scheuer, G. Paloczi, J. Poon, and A. Yariv. *Toward the Slowing and Storage of Light*. *OPN*, **16**, 36 (2005).
- [16] J. B. Khurgin. *Optical buffers based on slow light in electromagnetically induced transparent media and coupled resonator structures: comparative analysis*. *J. Opt. Soc. Am. B* **22**, #5, 1062(2005).
- [17] J. B. Khurgin. *Expanding the bandwidth of slow-light photonic devices based on coupled resonators*. *Optic Letters*, **30**, # 5, 513 (2005).
- [18] A. Yariv and Pochi Yeh. *Optical Waves in Crystals*. (“A Wiley-Interscience publication”, 1984).
- [19] A. Kuzmich, A. Dogariu, L. J. Wang, P. W. Milonni, R. Y. Chiao, *Phys. Rev. Lett.* **86**, 3925 (2001).
- [20] R. W. Boyd, D. J. Gauthier, in *Progress in Optics*, E. Wolf, Ed. (Elsevier, Amsterdam, 2002), vol. 43.
- [21] P. W. Milonni, *J. Phys. B* **35**, R31 (2002).
- [22] Matthew S. Bigelow, Nick N. Lepeshkin, and Robert W. Boyd. *Observation of Ultraslow Light Propagation in a Ruby Crystal at Room Temperature*. *Phys. Rev. Lett.* **90**, # 11, 113903 (2003).

- [23] Matthew S. Bigelow,* Nick N. Lepeshkin, Robert W. Boyd. *Superluminal and Slow Light Propagation in a Room-Temperature Solid*. Science, **301**, 200 (2003).
- [24] M. Yanik and S. Fan. *Stopping Light All Optically*. Phys. Rev. Lett. **92**, # 8, 083901, (2004).
- [25] M. Notomi,¹ K. Yamada,² A. Shinya,¹ J. Takahashi,² C. Takahashi,² and I. Yokohama. *Extremely Large Group-Velocity Dispersion of Line-Defect Waveguides in Photonic Crystal Slabs*. Phys. Rev. Lett. **87**, #25, 253902 (2001).
- [26] M. Scalora, R. J. Flynn, S. B. Reinhardt, R. L. Fork, M. J. Bloemer, M. D. Tocci, C. M. Bowden, H. S. Ledbetter, J. M. Bendickson, J. P. Dowling, R. P. Leavitt. *Ultrashort pulse propagation at the photonic band edge: Large tunable group delay with minimal distortion and loss*. Phys. Rev. E54, #2, R1078 (1996).
- [27] M. Bloemer, K. Myneni, M. Centini, M. Scalora, and G. D'Aguanno. *Transit time of optical pulses propagating through a finite length medium*. Phys. Rev. **E65**, 056615 (2002).
- [28] M. Soljacic, S. Johnson, S. Fan, M. Ibanescu, E. Ippen, and J. D. Joannopoulos. *Photonic-crystal slow-light enhancement of nonlinear phase sensitivity*. J. Opt. Soc. Am. B., **19**, #9, 2052 (2002).
- [29] A. Figotin, and I. Vitebskiy. *Electromagnetic unidirectionality in magnetic photonic crystals*. Phys. Rev. **B67**, 165210 (2003).
- [30] A. Figotin, and I. Vitebskiy. *Oblique frozen modes in layered media*. Phys. Rev. **E68**, 036609 (2003).
- [31] J. Ballato, A. Ballato, A. Figotin, and I. Vitebskiy. *Frozen light in periodic stacks of anisotropic layers*. Phys. Rev. **E71**, (2005).
- [32] A. Figotin and I. Vitebskiy. *Frozen light in photonic crystals with degenerate band edge*. Phys. Rev. **E74**, 066613 (2006)
- [33] A. Figotin and I. Vitebskiy. *Gigantic transmission band-edge resonance in periodic stacks of anisotropic layers*. Phys. Rev. **E72**, 036619, (2005).
- [34] A. Figotin and I. Vitebskiy. *Slow-wave resonance in periodic stacks of anisotropic layers*. Phys. Rev. **A76**, 053839 (2007)
- [35] A. Figotin and I. Vitebskiy. *Electromagnetic unidirectionality and frozen modes in magnetic photonic crystals*. JMMM, **300**, 117 (2006).
- [36] Pochi Yeh. "Optical Waves in Layered Media", (Wiley, New York, 1988).
- [37] Weng Cho Chew. "Waves and Fields in Inhomogeneous Media", (Van Nostrand Reinhold, New York, 1990).
- [38] M. Notomi. *Theory of light propagation in strongly modulated photonic crystals: Refractionlike behavior in the vicinity of the photonic band gap*. Phys. Rev. **B62**, 10696 (2000)
- [39] A. Figotin, and I. Vitebsky. *Nonreciprocal magnetic photonic crystals*. Phys. Rev. **E63**, 066609 (2001).

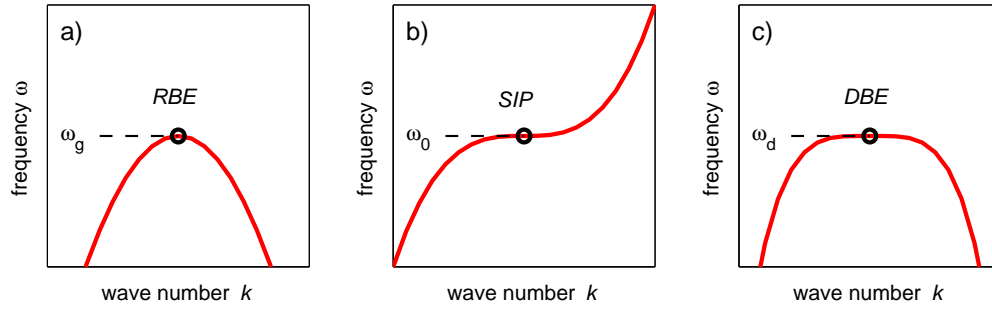


Figure 1. (Color online). Schematic examples of dispersion relations displaying different stationary points: (a) a regular band edge (RBE), (b) a stationary inflection point (SIP), (c) a degenerate band edge (DBE).

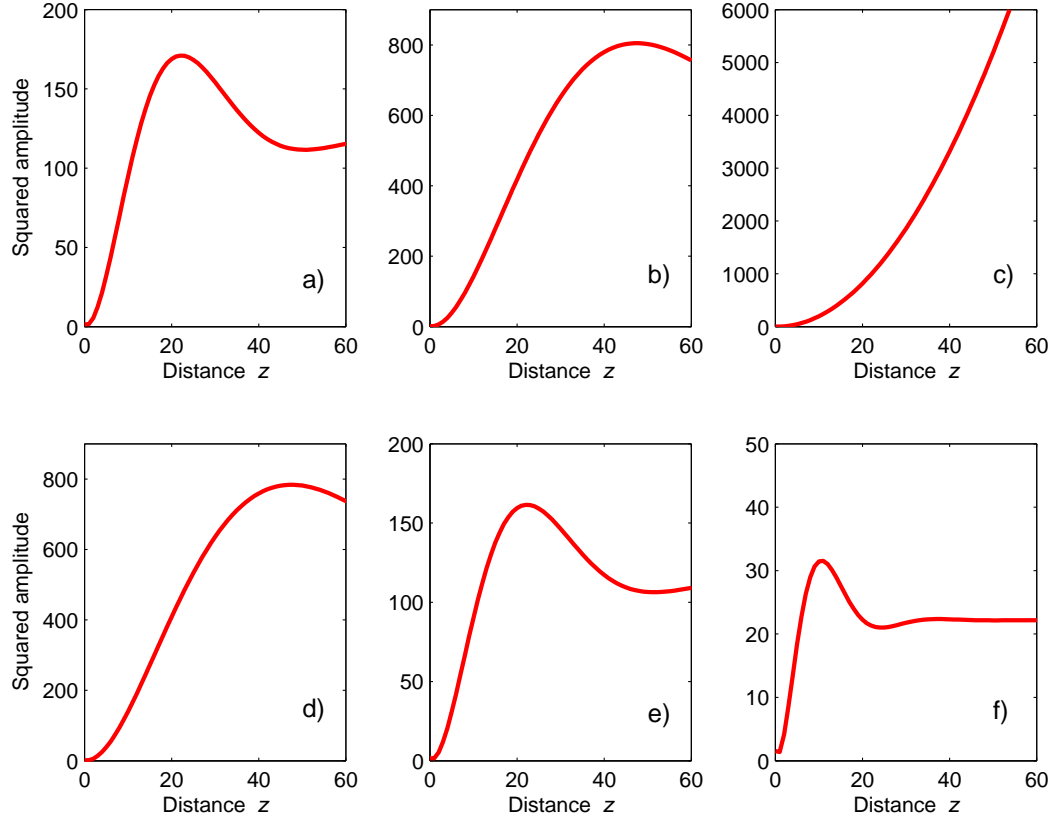


Figure 2. (Color online). Smoothed profile of the frozen mode at six different frequencies in the vicinity of stationary inflection point: (a) $\omega = \omega_0 - 10^{-4}c/L$, (b) $\omega = \omega_0 - 10^{-5}c/L$, (c) $\omega = \omega_0$, (d) $\omega = \omega_0 + 10^{-5}c/L$, (e) $\omega = \omega_0 + 10^{-4}c/L$, (f) $\omega = \omega_0 + 10^{-3}c/L$. In all cases, the incident wave has the same polarization and unity amplitude. The distance z from the surface of semi-infinite photonic crystal is expressed in units of L .

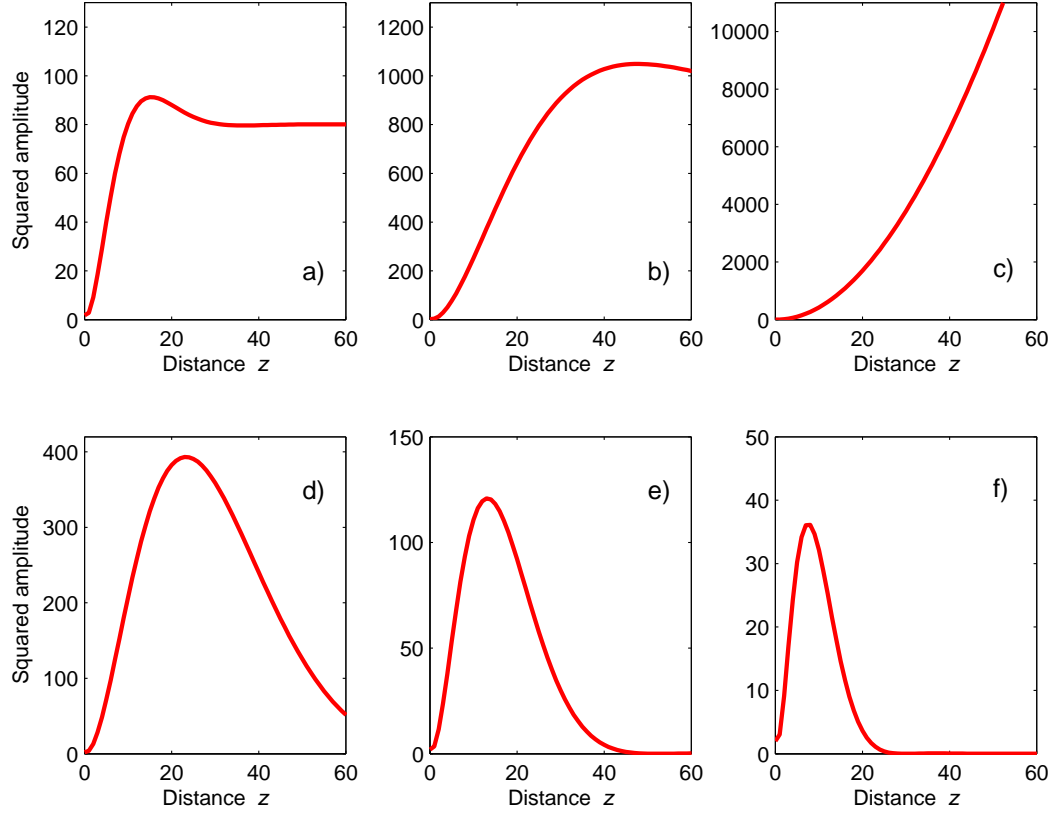


Figure 3. (Color online). Smoothed profile of the frozen mode at six different frequencies in the vicinity of degenerate band edge: (a) $\omega = \omega_d - 10^{-4}c/L$, (b) $\omega = \omega_d - 10^{-6}c/L$, (c) $\omega = \omega_d$, (d) $\omega = \omega_d + 10^{-6}c/L$, (e) $\omega = \omega_d + 10^{-5}c/L$, (f) $\omega = \omega_d + 10^{-4}c/L$. In the transmission band (at $\omega < \omega_d$), the asymptotic field value diverges as $\omega \rightarrow \omega_d$. By contrast, in the band gap (at $\omega > \omega_d$), the asymptotic field value is zero. The amplitude of the incident wave at $z < 0$ is unity. The distance z from the surface is expressed in units of L .

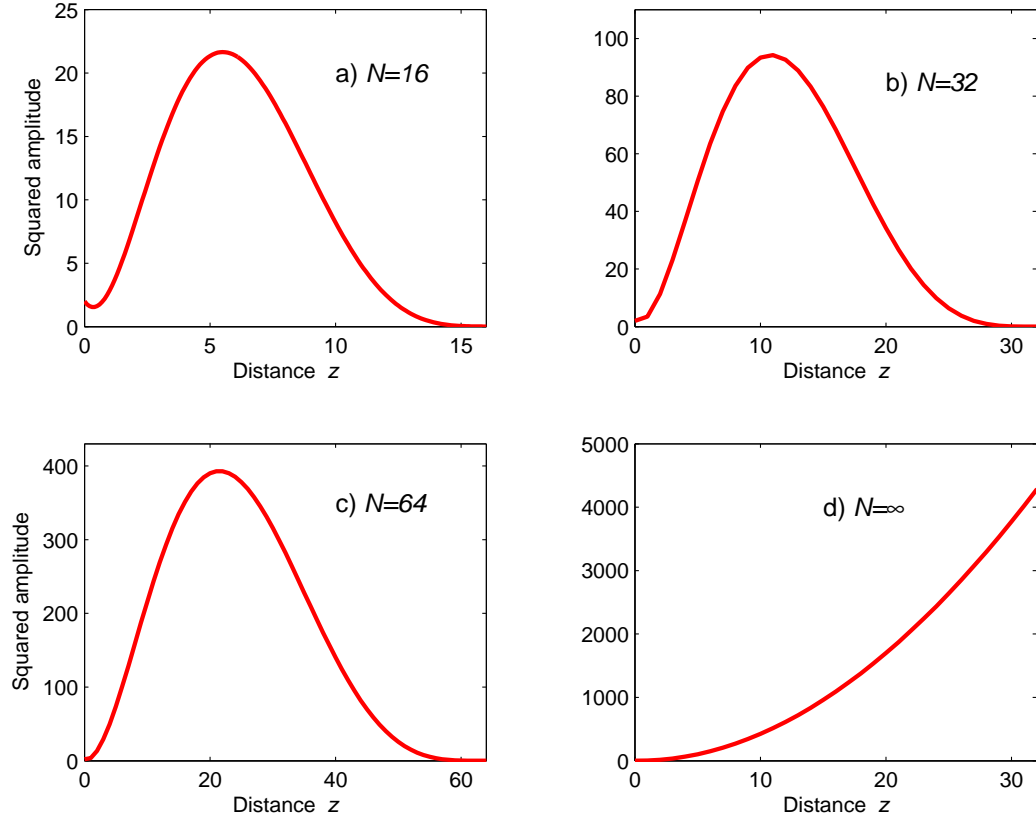


Figure 4. (Color online). Smoothed profile of the frozen mode in periodic layered structures composed of different number N of unit cells L . The frequency is equal to that of the degenerate band edge. The initial rate of growth of the frozen mode amplitude is virtually independent of N and described by (32). The limiting case (d) of the semi-infinite structure is also shown in Fig. 3(c). In all cases, the incident wave has the same polarization and unity amplitude. The distance z from the surface is expressed in units of L .

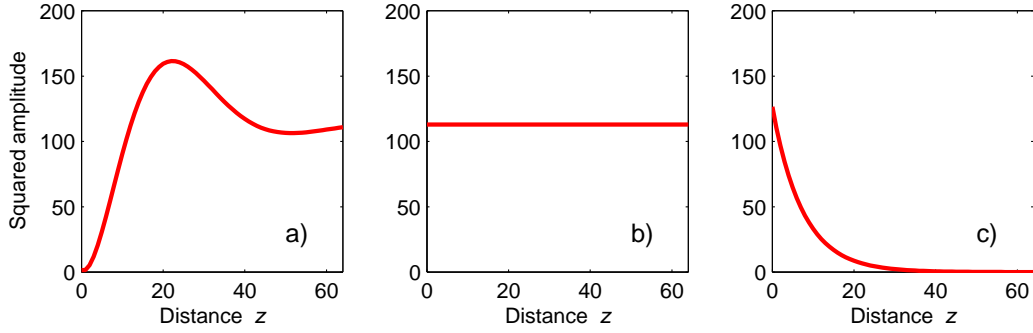


Figure 5. (Color online). Destructive interference of the propagating and evanescent components of the transmitted wave inside semi-infinite photonic crystal. The frequency is close but not equal to that of stationary inflection point. (a) The squared modulus of the resulting transmitted field – its amplitude at $z = 0$ is small enough to satisfy the boundary conditions (15); (b) the squared modulus of the propagating contribution, which is independent of z ; (c) the squared modulus of the evanescent contribution, which decays with the distance z . The amplitude of the incident wave is unity. The distance z from the surface is expressed in units of L .

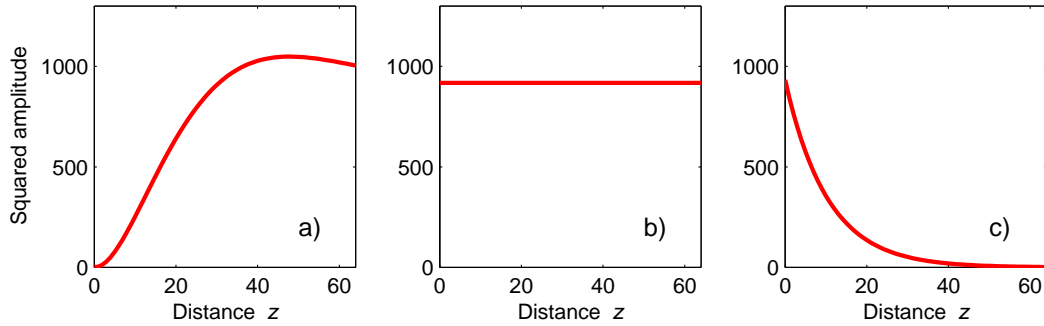


Figure 6. (Color online). Destructive interference of the two Bloch components of the transmitted wave inside semi-infinite photonic crystal. The frequency is $\omega = \omega_d - 10^{-4}c/L$, which is slightly below the degenerate band edge in Fig. ??(b). (a) The squared modulus of the resulting transmitted field – its amplitude at $z = 0$ is small enough to satisfy the boundary conditions (15); (b) the squared modulus of the propagating contribution, which is independent of z ; (c) the squared modulus of the evanescent contribution, which decays with the distance z . The amplitude of the incident wave is unity. Similar graphs related to the stationary inflection point are shown in Fig.5.

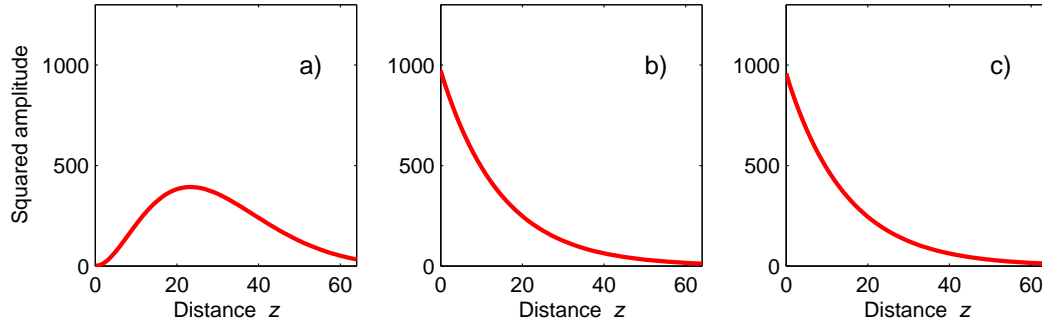


Figure 7. (Color online). Destructive interference of the two Bloch components of the transmitted wave inside semi-infinite photonic crystal. The frequency is $\omega = \omega_d + 10^{-5}c/L$, which is just above the degenerate band edge in Fig. ??(b). (a) The squared modulus of the resulting transmitted field – its amplitude at $z = 0$ is small enough to satisfy the boundary conditions (15); (b) and (c) the squared moduli of the two evanescent contributions; both decay with the distance z . The amplitude of the incident wave is unity. Similar graphs related to the frequency just below DBE in Fig. ??(b) are shown in Fig. 6.